JACS
JOURNAL OF THE AMERICAN CHEMICAL SOCIETY

Article

pubs.acs.org/JACS

Interconversion of η^3-H_2SiRR' σ-Complexes and 16-Electron Silylene Complexes via Reversible H−H or C−H Elimination

Mark C. Lipke, Felix Neumeyer, and T. Don Tilley*

Department of Chemistry, University of California, Berkeley, California 94720, United States

Supporting Information

ABSTRACT: Solid samples of η^3-silane complexes $[PhBP^{Ph}_3]$RuH(η^3-H_2SiRR') (R,R′ = Et_2, **1a**; PhMe, **1b**; Ph_2, **1c**, MeMes, **1d**) decompose when exposed to dynamic vacuum. Gas-phase H_2/D_2 exchange between isolated, solid samples of **1c-*d*$_3$** and **1c** indicate that a reversible elimination of H_2 is the first step in the irreversible decomposition. An efficient solution-phase trap for hydrogen, the 16-electron ruthenium benzyl complex $[PhBP^{Ph}_3]$Ru[η^3-CH_2(3,5-$Me_2C_6H_3$)] (**3**) reacts quantitatively with H_2 in benzene via elimination of mesitylene to form the η^5-cyclohexadienyl complex $[PhBP^{Ph}_3]$Ru(η^5-C_6H_7) (**4**). This H_2 trapping reaction was utilized to drive forward and quantify the elimination of H_2 from **1b,d** in solution, which resulted in the decomposition of **1b,d** to form **4** and several organosilicon products that could not be identified. Reaction of {$[PhBP^{Ph}_3]$Ru(μ-Cl)}$_2$ (**2**) with $(THF)_2Li(SiHMes_2)$ forms a new η^3-H_2Si species $[PhBP^{Ph}_3]$Ru[CH_2(2-(η^3-H_2SiMes)-3,5-$Me_2C_6H_2$)] (**5**) which reacts with H_2 to form the η^3-H_2SiMes_2 complex $[PhBP^{Ph}_3]$RuH(η^3-H_2SiMes_2) (**1e**). Complex **1e** was identified by NMR spectroscopy prior to its decomposition by elimination of Mes_2SiH_2 to form **4**. DFT calculations indicate that an isomer of **5**, the 16-electron silylene complex $[PhBP^{Ph}_3]$Ru(μ-H)(=$SiMes_2$), is only 2 kcal/mol higher in energy than **5**. Treatment of **5** with XylNC (Xyl = 2,6-dimethylphenyl) resulted in trapping of $[PhBP^{Ph}_3]$Ru(μ-H)(=$SiMes_2$) to form the 18-electron silylene complex $[PhBP^{Ph}_3]$Ru(CNXyl)(μ-H)(=$SiMes_2$) (**6**). A closely related germylene complex $[PhBP^{Ph}_3]$Ru[CN(2,6-diphenyl-4-MeC_6H_2)](H)(=GeH^tBu) (**8**) was prepared from reaction of ^{t}BuGeH_3 with the benzyl complex $[PhBP^{Ph}_3]$Ru[CN(2,6-diphenyl-4-MeC_6H_2)][η^1-CH_2(3,5-$Me_2C_6H_3$)] (**7**). Single crystal XRD analysis indicated that unlike for **6**, the hydride ligand in **8** is a terminal hydride that does not engage in 3c-2e Ru−H → Ge bonding. Complex **1b** is an effective precatalyst for the catalytic Ge−H dehydrocoupling of ^{t}BuGeH_3 to form (^{t}BuGeH_2)$_2$ (85% yield) and H_2.

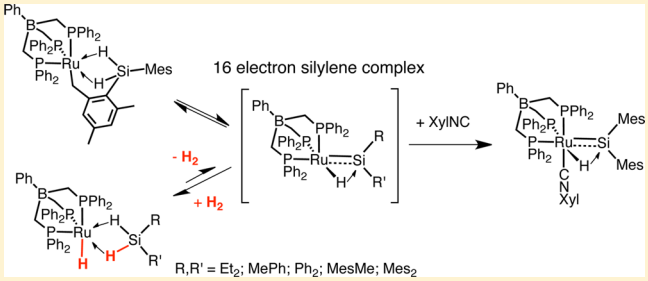

INTRODUCTION

Transition-metal silylene complexes are reactive species of considerable interest for their ability to participate in catalytic and stoichiometric Si−X (X = C, N, O, Si) bond-forming reactions.[1,2] Isolated silylene complexes exhibit reactivity with a wide range of nucleophilic substrates, and related species appear to participate as intermediates in catalytic transformations of silanes (e.g., silane dehydrocoupling and carbonyl hydrosilation).[3,4] Thus, it is important to demonstrate facile routes by which silylene complexes can form under catalytically relevant conditions. In this regard, it has been found that α-hydrogen elimination from a silyl ligand to an unsaturated metal center may generate a silylene complex, and this is one of the most general routes to species of this type.[5,6] This pathway requires an open coordination site at the metal center, which can be generated by reductive elimination of a C−H bond (Scheme 1, path A).[6] An analogous pathway involving elimination of an H−H bond (path B) could be important for generating reactive silylene intermediates *in situ* from hydrosilanes and inorganic precatalysts, but there are few examples of silylene complexes formed by this route.[7,8] The elimination of H_2 has been reported in the synthesis of [2,6-($CH_2P^tBu_2$)$_2$$C_6H_3$]Os(H)$_3$(=SiPhCl) from phenylsilane and [2,6-($CH_2P^tBu_2$)$_2$$C_6H_3$]Os(H)$_2$Cl,[8a] and for the formation of base-stabilized silylene complexes from silanes and carbonyl complexes (e.g., Fe(CO)$_5$, CpCo(CO)$_2$) under photolysis.[8b] Additionally, the formation of a related borylene complex (Cy_3P)$_2$Ru(H)(Cl)(=BMes) involves loss of H_2 from the η^3-H_2BMes complex (Cy_3P)$_2$Ru(H)(Cl)(η^3-H_2BMes).[9]

We recently reported that a family of η^3-H_2SiRR' σ-silane complexes $[PhBP^{Ph}_3]$RuH(η^3-H_2SiRR') (RR′ = Et_2, **1a**; MePh, **1b**; Ph_2, **1c**; MeMes, **1d**) are readily accessible by reaction of {$[PhBP^{Ph}_3]$Ru(μ-Cl)}$_2$ (**2**) with secondary silanes (Scheme 1).[10] Interestingly, crystalline samples of **1a−d** undergo spontaneous decomposition when exposed to dynamic vacuum, and this suggested that **1a−d** might reversibly eliminate H_2. Unusual 16-electron ruthenium silylene complexes are a possible product of H_2 elimination from **1a−d** (path C), and this would provide a convenient pathway to silylene complexes from a relatively simple inorganic coordination complex (note that **2** features only phosphine and chloride ligands). As

Received: February 20, 2014
Published: March 25, 2014

   dx.doi.org/10.1021/ja501803w | *J. Am. Chem. Soc.* 2014, 136, 6092−6102

Scheme 1. Pathways for Formation of Silylene Complexes

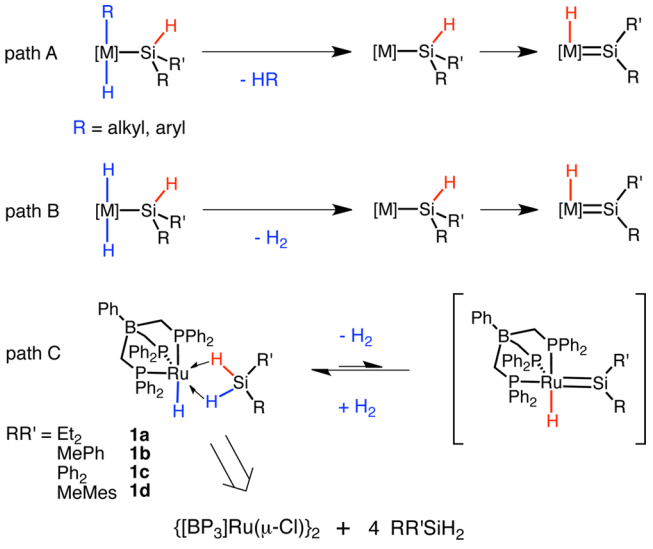

described below, investigation of this possibility led to synthesis of a new η^3-H_2Si species [PhBP$^{Ph}_3$]Ru[CH_2(2-(η^3-H_2SiMes)-3,5-$Me_2C_6H_2$)] (**5**) by reactions of $(THF)_2Li(SiHMes_2)$ with **2**. Complex **5** appears to exist in equilibrium with a 16-electron silylene complex [PhBP$^{Ph}_3$]Ru(μ-H)(=$SiMes_2$), as evident from DFT calculations and trapping of the silylene with XylNC to give the 18-electron silylene complex [PhBP$^{Ph}_3$]Ru(CNXyl)(μ-H)(=$SiMes_2$) (**6**). Additionally, treatment of **5** with H_2 results in the formation of [PhBP$^{Ph}_3$]RuH(η^3-H_2SiMes_2) (**1e**), in a process corresponding to the reverse of H_2 elimination from **1a**–**d**.

RESULTS AND DISCUSSION

Observed H_2 Elimination from 1a–d. Application of dynamic vacuum to crystalline samples of **1a**–**d** resulted in a color change from yellow to orange within 10 min. After a 24 h exposure to dynamic vacuum, samples of **1a**–**d** were dissolved in benzene-d_6 and analyzed by ^{1}H and ^{31}P{^{1}H} NMR experiments, which indicated the formation of multiple new organometallic products and the presence of unconverted **1a**–**d**. The decomposition appears to involve reversible elimination of a gas since **1a**–**d** are stable in solution (benzene-d_6) for at least 1 week in a sealed NMR tube and for at least 1 month as crystalline samples stored in a sealed container. Finely powdered samples of **1a**–**d** exhibited full decomposition after 2–5 days under dynamic vacuum. After dissolution in benzene-d_6, the major product was identified by ^{31}P{^{1}H} NMR spectroscopy (δ 39.5 ppm) as the cyclohexadienyl complex [PhBP$^{Ph}_3$]Ru(η^5-C_6D_6H) (**4**-d_6; see Scheme 2 for an independent synthesis). Minor organometallic products were detected by ^{31}P{^{1}H} NMR spectroscopy with resonances near 80 ppm, but these species could not be identified and were no longer observed after 12 h in solution.

A plausible decomposition pathway for **1a**–**d** involves the reversible elimination of H_2 as a first step. This possibility was supported by observation of H_2/D_2 exchange through the gas phase between powdered samples of **1c** and **1c**-d_3 that were separated within the same vessel and under static vacuum. After 5 days, the sample of **1c**-d_3 was examined by ^{1}H NMR spectroscopy (benzene-d_6), which revealed an Ru–H resonance that integrated as 0.5 H relative to the ligand backbone. This is an increase over the residual Ru–H resonance for the initial

Scheme 2

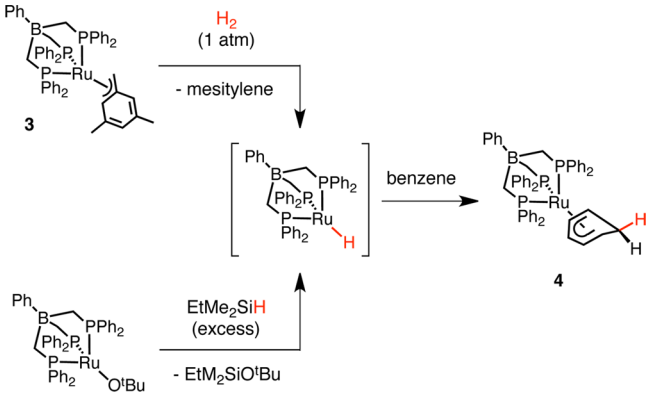

sample of **1c**-d_3 (0.15 H, Ru–H), indicating the exchange of H_2/D_2 through the gas phase.[11] The H_2 elimination appears to be followed by an irreversible decomposition, since **1a**–**d** could not be regenerated by exposure of the decomposition products to 1 atm of H_2 in the solid state or in solution.

The elimination of H_2 from solid samples of **1a**–**d** suggested that a similar process might occur in solution. However, observation of H_2 elimination from **1a**–**d** in solution proved difficult since the evaporation of suitable solvents (e.g., toluene, *o*-dichlorobenzene) under dynamic vacuum is considerably faster than the decomposition of these compounds.[12] Additionally, the equilibrium involving loss of H_2 appears to strongly favor the η^3-H_2SiRR′ complexes, as evidenced by a lack of decomposition for solutions of **1a**–**d** (in benzene-d_6) after five freeze–pump–thaw cycles (by ^{1}H and ^{31}P{^{1}H} NMR spectroscopy).

It was envisioned that the loss of H_2 from **1a**–**d** might be driven forward by use of a hydrogen trap, such as an unsaturated alkyl or aryl complex, that would rapidly and irreversibly react with H_2 to eliminate a hydrocarbon. To this end, **2** was treated with 1 equiv $(THF)_2MgMes_2$ in benzene, to provide the dark purple benzyl complex [PhBP$^{Ph}_3$]Ru[η^3-CH_2(3,5-$Me_2C_6H_3$)] (**3**, eq 1) that appears to result from

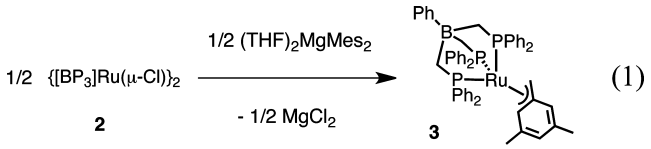

(1)

rearrangement of the unobserved intermediate [PhBP$^{Ph}_3$]Ru(Mes). Interestingly, **3** is a stable 16-electron η^3-benzyl complex and was identified by ^{1}H NMR (^{1}H δ 6.28 ppm, 1 H; 5.14 ppm, 2 H; 2.82 ppm, 2 H) and ^{13}C NMR resonances (^{13}C{^{1}H} δ 110.25 ppm; 37.48, q, J_{CP} = 6.4 Hz) that are consistent with a benzyl ligand exhibiting a coordinated π-system. An unsubstituted benzyl complex [PhBP$^{Ph}_3$]Ru[η^3-CH_2Ph], prepared from **2** and K[CH_2Ph], exhibits NMR data that are similar to those of **3**, but the unsubstituted benzyl complex is thermally unstable and could therefore not be isolated in pure form.[13]

The suitability of **3** as a trap for hydrogen was examined. Treatment of a solution of **3** (in benzene-d_6) with H_2 (1 atm) resulted in an immediate change in color from purple to pale yellow and quantitative formation of the cyclohexadienyl complex [PhBP$^{Ph}_3$]Ru(η^5-C_6D_6H) (**4**-d_6, by ^{1}H and ^{31}P{^{1}H} NMR spectroscopy, Scheme 2). The fully proteo isotopomer **4** was independently prepared and isolated via reaction of

dx.doi.org/10.1021/ja501803w | J. Am. Chem. Soc. 2014, 136, 6092–6102

Scheme 3. Use of 3 to Capture H_2 Eliminated from Solutions of η^3-H_2SiRR' Complexes

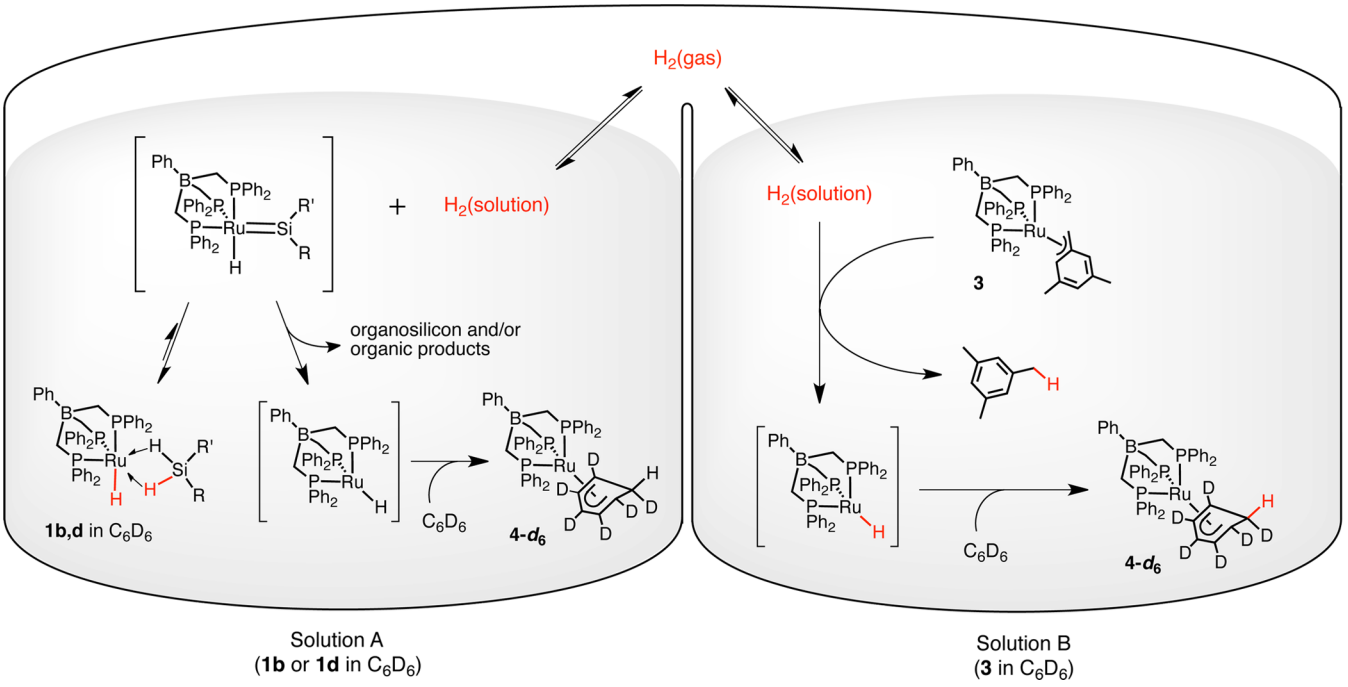

$[PhBP^{Ph}_3]Ru(O^tBu)$ with $EtMe_2SiH$ in benzene. The ^1H NMR spectrum for **4** displayed five resonances between 2.5−5.5 ppm that are indicative of the η^5-cyclohexadienyl ligand (^1H δ 5.32, 1 H; 5.11, 2 H; 2.90, 1 H; 2.72, 2 H; 2.67 ppm, 1 H).[14] The apical C−H resonance of the methylene group (2.67 ppm) appears as an approximate quintet ($J_{HH} \approx J_{PH} \approx 11$ Hz) in the ^1H NMR spectrum of **4** and as a doublet (J_{HH} = 12 Hz) in the $^1H\{^{31}P\}$ NMR spectrum. The other C−H resonances of the cyclohexadienyl ligand do not exhibit significant changes between the ^1H and $^1H\{^{31}P\}$ NMR spectra. For **4-d_6**, only the basal C−H resonance of the methylene group was observed for the cyclohexadienyl ligand (2.90 ppm, q, J_{PH} = 1.5 Hz). The formation of **4** is presumed to involve initial generation of the hydride species $[PhBP^{Ph}_3]RuH$, which may exist as a free 14-electron complex or as a 16-electron complex $[PhBP^{Ph}_3]Ru(H)L$ (e.g., where L = η^2-H−$CH_2C_6H_3Me_2$ or $EtMe_2SiO^tBu$). This reactive hydride species would then add to benzene, to give **4**. The closely related complex $[PhBP^{iPr}_3]Fe(\eta^5\text{-}C_6H_7)$ has previously been reported to form under related conditions that are consistent with addition of $[PhBP^{iPr}_3]FeH$ to benzene.[14]

The rapid and quantitative reaction of **3** with H_2 indicated that this benzyl complex might be suitable as a hydrogen acceptor for promoting and measuring the loss of H_2 from **1a−d** (Scheme 3). Thus, equimolar amounts of **3** and **1b** (each in 1 mL of benzene-d_6 with $(Me_3Si)_4Si$ internal standard) were stirred in separate glass bulbs that were connected via an evacuated headspace (Figure 1).[15] After 3 days, the dark purple solution of **3** had faded considerably in color and the yellow solution of **1b** had darkened to an orange-yellow color. Examination of these solutions by ^1H and $^{31}P\{^1H\}$ NMR spectroscopy revealed that **1b** had completely converted to several organometallic products, and the cyclohexadienyl complex **4-d_6** was the major product (85% yield). The sample of **3** had undergone 80% conversion to **4-d_6** and mesitylene as the only products, suggesting that **3** had reacted with most of the hydrogen expected from the elimination of H_2 from **1b**.

Figure 1. Apparatus for gas phase H_2 transfer from a solution of **1b,d** (yellow solution in right bulb) to a solution of **3** (purple solution in left bulb) through an evacuated headspace.[16]

To establish the origin of the hydrogen eliminated from **1b**, a deuterium-labeling experiment was conducted using **1b-d_3** for gas-phase D_2 transfer to **3**. After 3 days, the $^{31}P\{^1H\}$ NMR spectrum for the solution of **1b-d_3** (in benzene) revealed the complete consumption of **1b-d_3** and the formation of **4** as the major product. Interestingly, the ^2H NMR spectrum did not display a resonance for **4-d_1**, and thus **1b-d_3** appears to convert only to fully proteo **4** (see below for further discussion). Complex **3** had also been entirely consumed (by $^{31}P\{^1H\}$ NMR spectroscopy), and the ^2H NMR spectrum for this sample revealed resonances corresponding to **4-d_1** (^2H δ 2.85 ppm) and mesitylene-d_1 (^2H δ 2.13 ppm). By integration, these two products were formed in a 1:1 ratio, but they account for only 40% of the deuterium expected from elimination of 1 equiv of D_2 per mole of **1b-d_3** (determined by integration against a $Ph_2Si(CH_3)(CD_3)$ internal standard). An additional new ^2H resonance (^2H δ 7.38 ppm) was observed, which might result from incorporation of deuterium into a C−H position of the $[PhBP^{Ph}_3]$ ligand. This latter ^2H resonance accounts for an additional 40% of the expected deuterium, and this confirms

dx.doi.org/10.1021/ja501803w | J. Am. Chem. Soc. 2014, 136, 6092−6102

that **1b**-d_3 decomposed primarily through a pathway involving the elimination of D_2. These results demonstrate that reaction of **3** with H_2 offers an efficient method for trapping hydrogen and that this trapping reaction may be used to drive forward the equilibrium loss of hydrogen from **1b** (Scheme 3).

The initial product of H_2 elimination from **1b** (in benzene-d_6) could not be identified, but it seems possible that this species is the 16-electron silylene complex [PhBP$^{Ph}_3$]Ru(H)(=SiMePh). However, formation of the final product **4**-d_6 requires the additional loss of the SiMePh moiety. Several ^{1}H NMR resonances in the region 0.30−0.50 ppm (Si−CH_3 region) indicated the formation of new organosilicon products that could not be identified. Similarly, when using the η^3-H_2SiMeMes complex **1d** for the H_2 exchange experiment, multiple new Ar−CH_3 and Si−CH_3 resonances were observed in the ^{1}H NMR spectrum for the sample of **1d** after 2 days. Interestingly, in the deuterium-labeling experiment with **1b**-d_3 and **3** (in benzene), the C−D resonance for **4**-d_1 was not observed in the ^{2}H NMR spectrum after complete conversion of **1b**-d_3 to **4** nor were any other new ^{2}H NMR resonances observed for this solution. The formation of fully proteo **4** indicates that [PhBP$^{Ph}_3$]Ru−H, rather than [PhBP$^{Ph}_3$]Ru−D, is generated at some point after the elimination of D_2 from **1b**-d_3. Thus, the decomposition of an initially formed intermediate (e.g., [PhBP$^{Ph}_3$]Ru(D)(=SiMePh) or an isomer there of) must involve a C−H activation to provide the hydride (rather than deuteride) complex that subsequently reacts with benzene to form **4**. Since evidence for deuterium incorporation into the [PhBP$^{Ph}_3$] ligand was not observed in the ^{2}H NMR spectrum of this sample, the C−H activation might involve the C_6H_6 solvent or the SiMePh portion of the silane. These considerations imply that silylene complexes of this type are exceptionally reactive and therefore interesting synthetic targets for further investigation.

Evidence for a 16-Electron Silylene Complex. Given the possibility that the initial product of decomposition of **1a**−**d** is a 16-electron silylene complex of the type [PhBP$^{Ph}_3$]Ru(H)=SiRR′, attempts were made to develop an independent route to such species. Thus, the reaction of {[PhBP$^{Ph}_3$]Ru(μ-Cl)}$_2$ (**2**) with (THF)$_2$Li(SiHMes$_2$) was investigated as a possible route to a 14-electron Ru−SiHMes$_2$ silyl complex, which is expected to undergo α-H migration to form a 16-electron silylene hydride species.[5,17] Instead, this reaction (in benzene) resulted in formation of [PhBP$^{Ph}_3$]Ru[CH_2(2-(η^3-H_2SiMes)-3,5-$Me_2C_6H_2$)] (**5**), which is formed by intramolecular benzylic C−H activation, possibly involving an Ru−SiHMes$_2$ or Ru(H)=SiMes$_2$ intermediate (Scheme 4).[18] The structure of **5**, determined by single crystal XRD, features a benzylic ligand (d_{Ru-C} 2.209(3) Å) with a doubly agostic η^3-H_2SiMes substituent (d_{Ru-H} 1.72(3), 1.73(2) Å; d_{Si-H} 1.56(3) 1.58(2) Å) in the 2-position of the benzyl group (Figure 2). The η^3-H_2Si moiety is also indicated in the ^{1}H and ^{1}H−^{29}Si HMBC spectra, which display a Ru−H resonance (^{1}H δ −7.00 ppm) that features strong J-coupling with a downfield ^{29}Si signal (^{29}Si δ 138 ppm, J_{SiH} = 105 Hz).[10] Thus, **5** is closely related to **1a**−**d**, but **5** features a metalated benzyl group in place of the terminal hydride ligand in **1a**−**d**.

In order to determine if **5** is suitable as a model for the product of H_2 elimination from **1a**−**d**, the reverse reaction was examined by treatment of **5** with H_2 (1 atm in benzene-d_6, Scheme 5). This resulted in the complete consumption of **5** after 20 h and formation of [PhBP$^{Ph}_3$]RuH(η^3-H_2SiMes$_2$) (**1e**, 60%, Scheme 5), Mes$_2$SiH$_2$ (30%) and **4**-d_6 (30%, all yields

Scheme 4

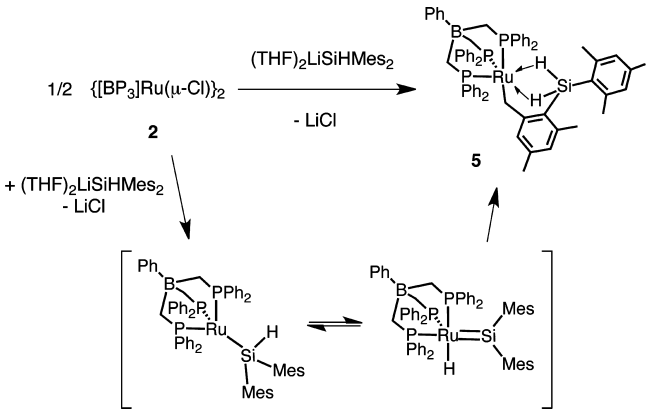

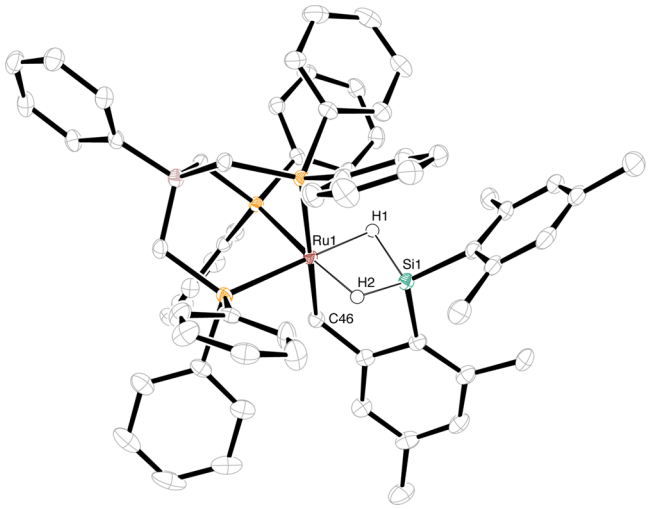

Figure 2. Solid-state structure of **5**, determined by single crystal XRD. Thermal ellipsoids are set to 50% probability, and nonhydridic hydrogen atoms are omitted for clarity.

Scheme 5

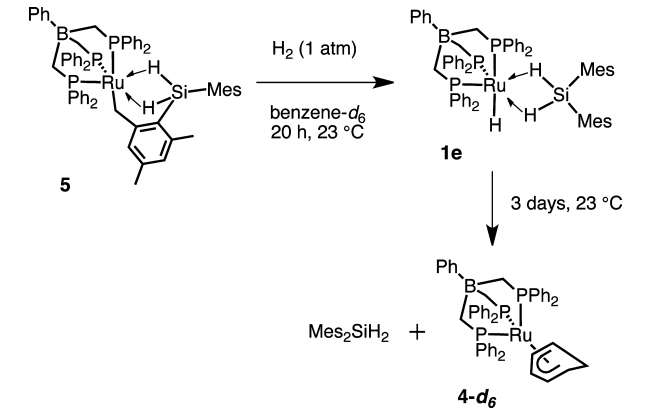

from ^{1}H and ^{31}P{^{1}H} NMR spectra). Complex **1e** is unstable to elimination of Mes$_2$SiH$_2$ (complete conversion to Mes$_2$SiH$_2$ and **4**-d_6 was observed after 3 days) and could not be isolated but was clearly identified from comparison of its NMR data to those of **1a**−**d**.[10] As with **1a**−**d** and **5**, the ^{29}Si−^{1}H HMBC NMR spectrum for **1e** displays a downfield ^{29}Si resonance (^{29}Si δ 131 ppm) that exhibits coupling to the Ru−H resonance (^{1}H δ −6.39 ppm, J_{SiH} = 65 Hz, 3 H; see Experimental Details for

dx.doi.org/10.1021/ja501803w | J. Am. Chem. Soc. 2014, 136, 6092−6102

additional NMR data). The formation of an η^3-H_2SiMes_2 complex from **5** is consistent with the reversible nature of H_2 loss from η^3-silane complexes **1a–d**. The elimination of hydrogen was not directly observed in the case of **1e** due to decomposition by a different route (loss of Mes_2SiH_2). However, the observation of H_2 elimination from the closely related complexes **1a–d** strongly suggests that **1e** might exist in equilibrium with H_2 and **5**.

It seemed possible that **5** might exist in equilibrium with the silylene complex [PhBP$^{Ph}_3$]Ru(H)=SiMes$_2$ (**Int A**, Scheme 6)

Scheme 6

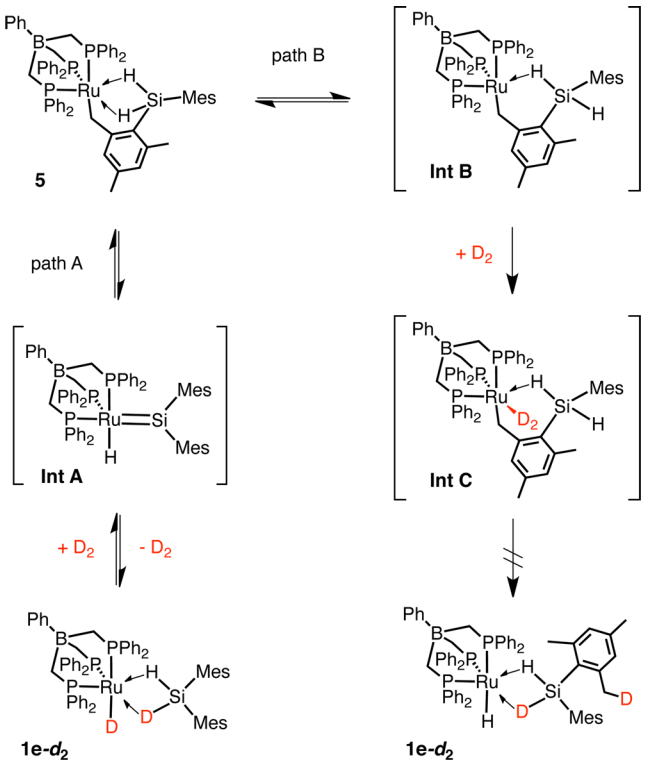

and that this latter species is an intermediate in the reaction of **5** with H_2 to form **1e** (path A). The silylene species could possibly form via C–H elimination from **5** in a process related to the H–H elimination observed for **1a–d**. However, it is also possible that the formation of **1e** from **5** involves binding of H_2 to ruthenium prior to C–H elimination (path B). To distinguish between these possibilities, a labeling experiment was conducted by treatment of **5** with D_2 (1 atm, in benzene or benzene-d_6, Scheme 6). For path A, deuterium should be incorporated only into the Ru–D and Ru–D–Si positions upon formation of **1e-d_2** since the benzylic C–H bond forms prior to the addition of D_2. For path B, deuterium incorporation should be 1:1 for the Ru–D and benzylic C–D positions since the small η^2-D_2 ligand of **Int C** should more rapidly participate (relative to the geometrically constrained η^2-H–Si ligand) in an oxidative addition/reductive elimination process or a σ-bond metathesis process with the Ru–CH_2Ar group.

The results of the deuterium-labeling experiment were more complicated than initially envisioned (presumably due to reversibility of the benzylic C–H bond formation) but indicate that **1e-d_2** forms via path A. Three hours after addition of D_2 (1 atm) to a solution of **5** (in benzene), an Ru–D resonance for **1e-d_2** was clearly observed by ^{2}H NMR spectroscopy, while only slight incorporation of deuterium into the benzylic C–D position was evident (ratio of C–D to Ru–D ≤ 1:5). The ratio of C–D to Ru–D increased to 1:3 after 6 h and to 1:2 after 20 h. After 3 days, the dimesitylsilane product resulting from decomposition of **1e** was isolated and found to have a 1.6:10.4 ratio of C–D to C–H in the *ortho* benzylic methyl positions (by ^{1}H and ^{2}H NMR). The incorporation of more than one deuterium atom (per molecule of Mes_2SiH_2) into these positions indicates that formation of the benzylic C–H bond in **1e** is reversible, thus allowing deuterium to exchange into this position after the initial formation of **1e-d_2**. Note that this observation is consistent with the expectation that **1e** might exist in equilibrium with **5** and H_2. Since deuterium incorporation into the Ru–H(D) positions is initially much faster than for the C–H(D) positions, this labeling experiment provides evidence that the C–H bond is formed prior to the addition of D_2 in the initial conversion of **5** to **1e-d_2**. This provides support for the existence of the 16-electron silylene complex [PhBP$^{Ph}_3$]Ru(H)(=SiMes$_2$) (**Int A**) as an intermediate in the formation of **1e-d_2** from **5** (path A). Note, however, that these results cannot rule out the possibility that a closely related 14-electron silyl complex [PhBP$^{Ph}_3$]Ru–SiHMes$_2$ (see Scheme 4) is actually the key intermediate responsible for D–D activation to form **1e-d_2** or C–H activation to revert back to **5**. Regardless, the 14-electron silyl complex would be expected to exist in equilibrium with the 16-electron silylene complex **Int A**, and thus these results suggest that both **5** and **1e** appear to exist in equilibrium with the 16-electron silylene hydride complex [PhBP$^{Ph}_3$]Ru(H)(=SiMes$_2$).

It seemed possible that [PhBP$^{Ph}_3$]Ru(H)(=SiMes$_2$) might be trapped by the binding of a ligand to the ruthenium center, the silicon center, or both. Thus, complex **5** was dissolved in THF-d_8, a potential ligand for silicon,[19] and the solution was monitored by ^{1}H and ^{31}P{^{1}H} NMR spectroscopy. After 1 week, partial decomposition of **5** was observed (by ^{1}H NMR spectroscopy) to form products that could not be identified. The isocyanide XylNC was examined as a trap for the 16-electron silylene complex, by addition of 1 equiv to a benzene-d_6 solution of **5**. This resulted in formation of the 18-electron silylene complex [PhBP$^{Ph}_3$]Ru(CNXyl)(μ-H)(=SiMes$_2$) (**6**, Scheme 7) after 4 h at room temperature (in benzene-d_6, by ^{1}H and ^{31}P{^{1}H} NMR spectroscopy).

Silylene complex **6** was examined to provide possible insight into the structure of the 16-electron silylene species from which **6** is derived. The solid-state structure of **6** was determined by single crystal XRD (Figure 3), including the location and

Scheme 7

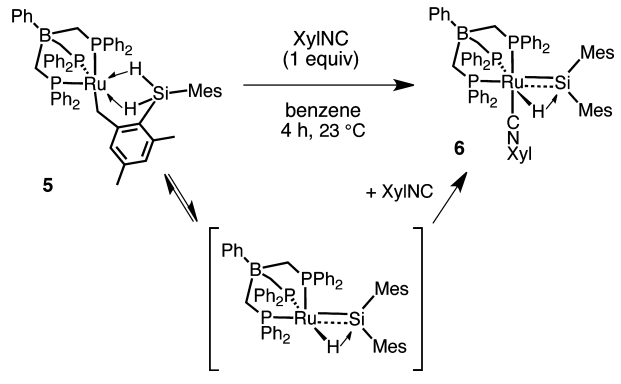

dx.doi.org/10.1021/ja501803w | J. Am. Chem. Soc. 2014, 136, 6092–6102

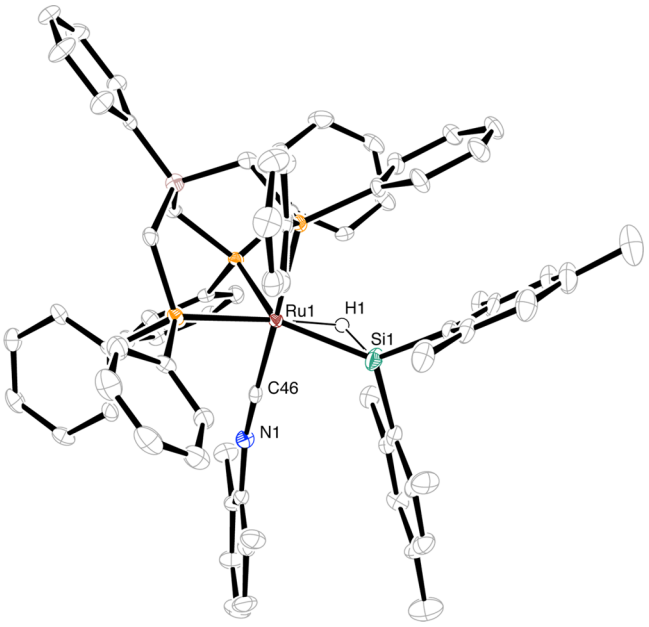

Figure 3. Structure of **6** determined by single crystal XRD analysis. Thermal ellipsoids are set to 50% probability, and nonhydridic hydrogen atoms are omitted for clarity.

refinement of the bridging hydride position.[6c,20] The ruthenium center exhibits an approximate trigonal bipyramidal coordination geometry, with the hydride ligand occupying an additional position that bridges the Ru=Si double bond. Silylene character is indicated by planarity of the silicon, ruthenium, and *ipso* carbons of the mesityl groups (sum of bond angles at Si = 359.9(2)°). The Ru−H and Si−H distances (d_{Ru-H} 1.53(6) Å, d_{Si-H} 1.17(5) Å) are unrealistically short[21] but suggest the hydride is bridging between ruthenium and silicon. Notably, the Ru−Si distance (2.299(2) Å) is unusually long for a silylene complex,[22] which may be due to the steric bulk of both the [PhBP$^{Ph}_3$] ligand and the $SiMes_2$ fragment.

The ^{1}H NMR spectrum for **6** contains an Ru−H resonance that exhibits coupling to three inequivalent phosphorus atoms (^{1}H δ −7.92 ppm, J_{PH} = 32, 9, 3 Hz). In the ^{1}H{^{31}P} NMR spectrum, the Ru−H resonance appears as a singlet with visible satellites from coupling to silicon-29 (J_{SiH} = 43 Hz), which confirms the presence of an Ru−H→Si interaction. The ^{1}H−^{29}Si HMBC NMR spectrum displays the Ru−H resonance as coupled to a downfield ^{29}Si resonance (^{29}Si δ 208 ppm) that is consistent with the presence of a silylene ligand in **6**.[1b,7] Thus, **6** is best described as a silylene complex in which the empty p orbital on silicon is stabilized by donation from the hydride ligand.[6c,20] This bonding description is supported by a DFT structural optimization that produced Ru−H and Si−H distances that indicate the hydride has significant bonding interactions with both the ruthenium and silicon centers (d_{Ru-H} 1.78 Å, d_{Si-H} 1.70 Å for **6-DFT**).[23]

The presence of a Ru−H→Si dative interaction in **6** suggested that the corresponding 16-electron silylene complex might also feature a bridging hydride. The structure **6-DFT** was used as a starting point for performing DFT calculations on the analogous, 16-electron silylene complex [PhBP$^{Ph}_3$]Ru(μ-H)=$SiMes_2$.[23] The XylNC ligand was deleted from **6-DFT**, followed by a geometry optimization calculation that provided the structure **silylene-DFT** (Figure 4a). This structure features a Ru(μ-H)=$SiMes_2$ moiety that is similar to that of **6-DFT** (d_{Ru-H} 1.78 Å, d_{Si-H} 1.72 Å for **silylene-DFT**). Additionally, there is an agostic interaction between a benzylic C−H bond and the unsaturated ruthenium center ($d_{Ru-H,agostic}$ 1.94 Å). Interestingly, these calculations found that **silylene-DFT** is only 2 kcal/mol higher in free energy than **5-DFT**, and this small energy difference is consistent with experimental results that suggest that the 16-electron silylene complex is readily accessible from **5**.

Notably, there are few examples of silylene complexes that are unsaturated at the metal center, and this unsaturation may promote reactivity that is not possible for most silylene complexes.[2e,24] For example, a 16-electron titanium silylene complex has been implicated as a key intermediate in an unusual [2 + 2] cycloaddition with alkynes.[2e] The molecular orbitals predicted for **silylene-DFT** were examined to gain insight into the bonding of this unusual species and the relative accessibility of the two available acceptor orbitals. The HOMO is a distorted Ru=Si π-bonding orbital, similar to those reported for other M(μ-H)=SiR_2 species (see Supporting Information).[20] The LUMO is the corresponding π^*-orbital (Figure 4b), which has a large contribution from a silicon 3p orbital as is typical for silylene complexes.[25] The LUMO +1 is the σ^* combination of a phosphine ligand, a ruthenium 4d orbital, and the agostic C−H bond (Figure 4c). Thus, silylene complexes of this type feature two unoccupied orbitals (at both the ruthenium and silicon centers) that should be accessible to nucleophiles.

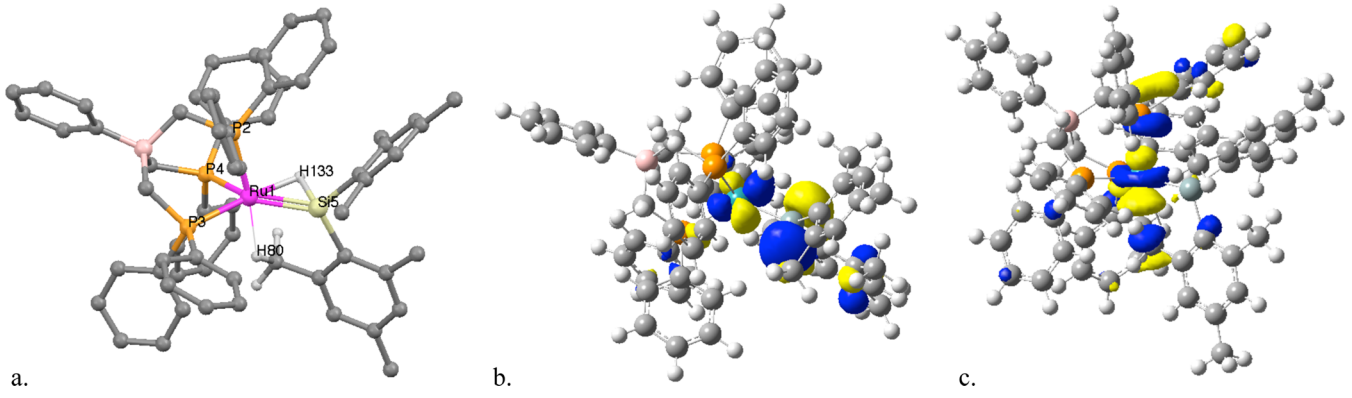

Figure 4. (a) Structure of **silylene-DFT** determined by DFT geometry optimization. Representation of the (b) LUMO and (c) LUMO + 1 of **silylene-DFT**.

dx.doi.org/10.1021/ja501803w | J. Am. Chem. Soc. 2014, 136, 6092−6102

Facile H_2 Elimination Involving Hydridogermanes. It was anticipated that the [PhBP$^{Ph}_3$]Ru fragment might support germylene or η^3-H_2GeRR′ complexes, and efforts were focused on preparing and isolating such species for comparison with the related σ-silane complexes **1a**–**d** and the silylene complex **6**. Complexes **1a**–**c** rapidly undergo silane exchange with free silanes (e.g., formation of **1b** from treatment of **1a** with excess $PhMeSiH_2$), and it seemed possible that the silanes in **1a**–**c** might also be displaced by hydridogermanes to form η^3-H_2GeRR′ complexes. Treatment of **1c** with excess Ph_2GeH_2 (10 equiv) resulted in displacement of the silane within 30 min and formation of H_2 and multiple organometallic species that could not be identified (by ^{1}H and ^{31}P{^{1}H} NMR spectroscopy). Upon treatment of **1b** with ^{t}BuGeH$_3$, the elimination of H_2 was also observed (by ^{1}H NMR spectroscopy), but in this case the H_2 elimination facilitated a catalytic cycle for Ge–H dehydrocoupling[3] to form (^{t}BuGeH$_2$)$_2$ (determined by ^{1}H NMR spectroscopy and GC-MS, eq 2). Using 1 mol % of **1b**,

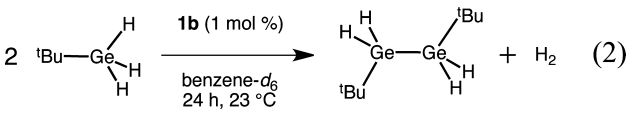

(2)

the reaction provided an 85% yield of the digermane after 24 h at room temperature (by ^{1}H NMR spectroscopy). In contrast, dehydrocoupling was not observed for Ph_2GeH_2 under these conditions, even though H_2 elimination was detected by ^{1}H NMR spectroscopy.

Considering the ability of **1a**–**d** to eliminate hydrogen, it is conceivable that a related complex [PhBP$^{Ph}_3$]Ru(H)(η^3-H_2GeH^{t}Bu) is responsible for the H_2 elimination step of the Ge–H dehydrocoupling reaction (Scheme 8). Notably,

Scheme 8. Potential Mechanism for the Homo-Dehydrocoupling of ^{t}BuGeH$_3$

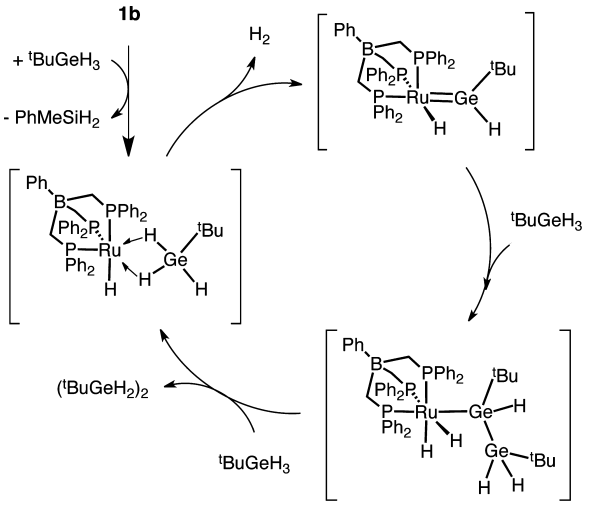

$PhMeSiH_2$ was observed (by ^{1}H NMR spectroscopy) as a free species after the addition of ^{t}BuGeH$_3$ to **1b**, and this is consistent with displacement of the silane ligand by the germane. The elimination of H_2 from the resulting η^3-H_2GeH^{t}Bu complex might produce a 16-electron germylene complex [PhBP$^{Ph}_3$]Ru(H)(=GeH^{t}Bu) that could conceivably react with an equivalent of ^{t}BuGeH$_3$ to engage in Ge–H bond activation and Ge–Ge bond formation.[3,26] Multiple Ru–H resonances were observed in the ^{1}H NMR spectrum of this reaction mixture, and the corresponding complexes could not be identified. Thus, the possible involvement of an η^3-H_2GeH^{t}Bu species in this Ge–H dehydrocoupling reaction remains speculative but is consistent with the reactivity observed for the [PhBP$^{Ph}_3$]Ru fragment with silanes (i.e., silane–silane exchange reactions involving **1a**–**c**, and the elimination of H_2 from **1a**–**d**).

Since neither η^3-H_2GeRR′ complexes nor germylene complexes could be identified upon treatment of **1a**–**d** with gemanes, efforts to prepare germylene complexes were focused on reactions of germanes with the benzyl complex **3** or the related isocyanide complex [PhBP$^{Ph}_3$]Ru[CN(2,6-diphenyl-4-MeC$_6$H$_2$)][CH$_2$(3,5-Me$_2$C$_6$H$_3$)] (**7**). Multiple products were obtained upon reactions of **3** with Ph_2GeH_2 or ^{t}BuGeH$_3$, and these could not be isolated. Similarly, silylene complexes could not be obtained by treatment of either **3** or **7** with silanes (e.g., $PhSiH_3$, $MesSiH_3$, $PhMeSiH_2$, Ph_2SiH_2, $MesMeSiH_2$). However, treatment of **7** with ^{t}BuGeH$_3$ resulted in elimination of mesitylene and formation of the hydridogermylene complex [PhBP$^{Ph}_3$]Ru[CN(2,6-Ph$_2$-4-MeC$_6$H$_2$)](H)=GeH^{t}Bu (**8**, eq 3). The ^{1}H NMR spectrum for **8** displays a broad resonance

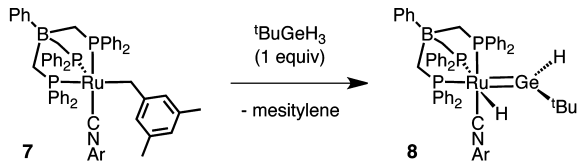

(3)

at 10.75 ppm that is consistent with the Ge–H hydrogen of a M=Ge(H)^{t}Bu complex.[27] The Ru–H ^{1}H NMR resonance (−8.36 ppm) is similarly quite broad, and thus the Ru–H and Ge–H hydrogens appear to readily exchange at room temperature. At −30 °C, both the Ru–H and Ge–H resonances appear as sharp signals that each integrate as 1 H.

The solid-state structure of **8** was determined by single crystal XRD, including location and refinement of the Ru–H and Ge–H hydrogen atoms (Figure 5). Germylene character is indicated by planarity about germanium (sum of bond angles at Ge = 359.8(9) Å) and the short Ru–Ge distance (d_{Ru-Ge}

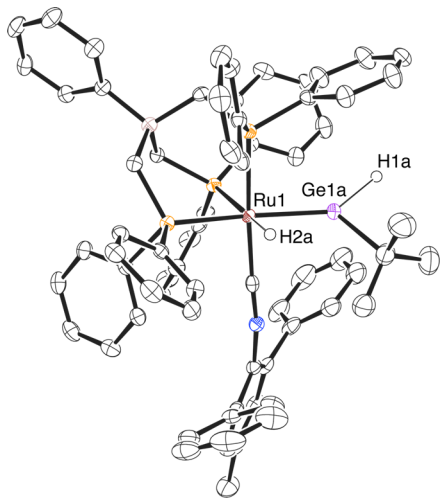

Figure 5. Solid-state structure of **8** determined by single crystal XRD analysis. Ellipsoids are set to 50% probability, and C–H hydrogen atoms are omitted for clarity.

dx.doi.org/10.1021/ja501803w | J. Am. Chem. Soc. 2014, 136, 6092–6102

2.3377(4) Å).[27] Interestingly, this Ru−Ge distance is only 1.7% longer than the Ru−Si distance in **6** despite an 8% increase in covalent radius between silicon and germanium.[28] The structure of **8** exhibits other notable differences with **6**, and these include the absence of a bridging Ru−H→Ge interaction. The GeH^tBu plane is oriented such that donation from the hydride ligand into the germanium p orbital is not possible. The absence of a Ru−H→Ge interaction in **8** is also evident from the long Ge−$H_{hydride}$ distance ($d_{Ge-H(hydride)}$ 2.45(4) Å) and a coordination geometry for ruthenium that is much closer to octahedral (vs that for **6**).

Hydrogen forms stronger bonds to silicon than to germanium,[29] and this may explain the structural differences between **8** and **6** as well as the relative ease with which hydrogen is eliminated in the catalytic Ge−H dehydrocoupling reaction observed for $^tBuGeH_3$. The structural differences between **8** and **6** may also be influenced by the much larger size of the $SiMes_2$ group relative to the GeH^tBu group, which allows the GeH^tBu ligand to approach a *cis*-phosphine group more closely than does the $SiMes_2$ group in **6** (P_{cis}−Ru−Ge angle =108.03(2)°, **8**; P_{cis}−Ru−Si angle =144.76(5)°, **6**). The small hydrogen substituent also allows a conformation for the GeH^tBu group that involves a nearly coplanar arrangement with the Ru−H bond (H−Ru−Ge−C dihedral angle = 29(1)°). For the corresponding 16-electron germylene complex, this orientation of the Ge^tBuH group would result in a parallel alignment of the p orbital on germanium with the acceptor orbital centered on ruthenium. This could be important for facilitating addition of a Ge−H bond across the Ru═Ge bond, as proposed for the catalytic dehydrocoupling of $^tBuGeH_3$ (Scheme 8). This is consistent with the absence of dehydrocoupling reactivity for Ph_2GeH_2 using **1b** as a precatalyst since the larger $GePh_2$ fragment may be unable to adopt the necessary conformation.

CONCLUSION

The η^3-H_2SiRR′ complexes **1a−d** were found to eliminate H_2, apparently in an equilibrium between **1a−d** and 16-electron silylene complexes [$PhBP^{Ph}_3$]Ru(μ-H)═SiRR′. These silylene complexes are unstable to further decomposition and could not be directly observed; thus, a related η^3-H_2Si species ([$PhBP^{Ph}_3$]Ru[CH_2(2-(η^3-H_2SiMes)-3,5-$Me_2C_6H_3$] (**5**) was prepared as a model for the product of H_2 elimination from **1a−d**. Notably, complex **5** exists in equilibrium with the 16-electron silylene complex ([$PhBP^{Ph}_3$]Ru(μ-H)═$SiMes_2$), which was trapped with XylNC to form the 18-electron silylene complex **6**. The equilibrium between **5** and [$PhBP^{Ph}_3$]Ru(μ-H)═$SiMes_2$ involves a reversible C−H elimination analogous to the H−H elimination from **1a−d**. This provides support for the possibility of an equilibrium between **1a−d** and 16-electron silylene complexes similar to [$PhBP^{Ph}_3$]Ru(μ-H)═$SiMes_2$. Notably, silylene complexes with an unsaturated metal center are uncommon, and previously detected or isolated examples involved transition-metal centers that are relatively amenable to having fewer than 18-electrons (e.g., group 4 metals,[2e,24a] square planar Pt(II)[5a] or Ni(II),[17] and linear Pd(0)[24b]).

The equilibrium between **1a−d** and unsaturated silylene complexes is particularly remarkable since **1a−d** are formed from the treatment of a simple inorganic coordination complex {[$PhBP^{Ph}_3$]Ru(μ-Cl)}$_2$ (**2**) with hydridosilanes. This demonstrates a simple pathway by which reactive silylene complexes might be formed as transient intermediates from common inorganic precatalysts (e.g., $(Ph_3P)_3RuCl_2$). Such processes could have particular relevance to dehydrocoupling reactions as evidenced by the possible role of η^3-H_2GeRR′ species in the hydrogen elimination step of a Ge−H dehydrocoupling reaction. It is notable that the [$PhBP^{Ph}_3$]Ru fragment can support a variety of silylene complexes and related species (i.e., η^3-silane complexes and germylene complexes). This will allow for detailed comparisons of the reactivity of these species with each other, as well as with the reactivity of previously studied Ru═ER_2 (E = Si, Ge, Sn) complexes.

EXPERIMENTAL DETAILS

General Considerations. All manipulations of air-sensitive compounds were conducted under a nitrogen atmosphere using standard Schlenk techniques or using a nitrogen atmosphere glovebox. Proteo solvents were stored in PTFE-valved flasks after drying using vacuum atmosphere solvent purification systems or by distillation under nitrogen from appropriate drying agents. Deuterated solvents (Cambridge Isotopes) were dried over NaK and vacuum transferred prior to use. Xylyl isocyanide was purchased from commercial sources and purified by sublimation prior to use. The reagents $(THF)_2$Li-$(SiHMes_2)$,[30] $(THF)_2MgMes_2$,[31] and 2,6-diphenyl-4-methylphenyl isocyanide[32] were prepared according to literature procedures. The complexes {[$PhBP^{Ph}_3$]Ru(μ-Cl)}$_2$,[33] [$PhBP^{Ph}_3$]RuO^tBu,[34] and [$PhBP^{Ph}_3$]RuH(η^3-H_2SiRR′) (R,R′ = Me,Ph **1b**; RR′ = Ph_2 **1c**)[10] were prepared as previously reported. Samples of **1b,c-d_3** were prepared by the same procedure as **1b,c** but using $PhMeSiD_2$ or Ph_2SiD_2. The $^{31}P\{^1H\}$ and ^1H NMR spectra of **1b,c-d_3** were identical to those of **1b,c** except for the absence of a significant Ru−H resonance in the ^1H NMR spectra of **1b,c-d_3**.

NMR spectra were recorded on Bruker spectrometers at room temperature unless otherwise noted. Spectra were referenced internally by the residual proton signal relative to tetramethylsilane for ^1H NMR, the residual solvent ^2H NMR peaks for ^2H NMR, solvent peaks for $^{13}C\{^1H\}$ NMR, external 85% H_3PO_4 for $^{31}P\{^1H\}$ NMR, and tetramethylsilane for $^{29}Si-^1H$ HMBC experiments. Assignment of certain $^{13}C\{^1H\}$ NMR signals was made on the basis of $^1H-^{13}C$ HSQC NMR data. The $^{13}C\{^1H\}$ NMR spectra for compounds **3−8** feature some broad and/or overlapping resonances so that each individual peak in the aromatic region could not be observed or individually indentified. The J_{SiH} values for Ru−H−Si resonances were determined by examining satellite signals around the main Ru−H resonance in $^1H\{^{31}P\}$ NMR spectra or by the Ru−H resonances displayed in ^{29}Si-filtered $^1H\{^{31}P\}$ NMR experiments. Infrared spectra (Nujol mulls on NaCl plates) were recorded using a Nicolet 6700 FTIR spectrometer at a resolution of 2 cm^{-1}. XRD data were collected on a Bruker Platform goniometer with a charge coupled device (CCD) detector (Smart Apex). Structures were solved using the SHELXTL (version 5.1) program library (G. Sheldrick, Bruker Analytical X-ray Systems, Madison, WI). All software and sources of scattering factors are contained in the SHELXTL (version 5.1) program library; G. Sheldrick, Bruker Analytical Systems, Madison, WI. Elemental analyses were performed by the University of California, Berkeley College of Chemistry Microanalytical Facility.

Synthesis of [$PhBP^{Ph}_3$]RuH(η^3-H_2SiEt_2) (1a). A solution of Et_2SiH_2 (48 mg, 0.544 mmol) in 5 mL of fluorobenzene was added to a vial containing solid **2** (147 mg, 0.089 mmol). The orange suspension was stirred for 2 h, resulting in a dark amber solution. The reaction solution was filtered, layered with 10 mL of pentane, and cooled to −35 °C. After 5 days, yellow crystals of **1a** were isolated from the mixture, washed with pentane (3 × 2 mL), and dried under a gentle stream of nitrogen, providing analytically pure **1a** (80 mg, 51%). Anal. calcd for $C_{49}H_{54}BSiP_3Ru$ (875.86): C, 67.20; H, 6.21. Found: C, 67.47; H, 6.05. ^1H NMR (C_6D_6, 600 MHz): δ 8.19 (br d, J = 7.1 Hz, 2 H), 7.70 (t, J = 7.4 Hz, 2 H), 7.58 (br, 12 H), 7.44 (tt, J = 7.4, 1.3 Hz, 1 H), 6.82−6.87 (m, 18 H), 1.86 (br, 6 H, ($B(CH_2PPh_2)$), 1.01 (t, J = 7.5, 6 H), 0.91−0.97 (m, 4 H), −7.40 (m, J_{SiH} = 64 Hz, 3 H, Ru−H). $^{13}C\{^1H\}$ NMR (C_6D_6, 150.893 MHz): 163.75, 142.35 (m), 132.03, 131.88 (m), 129.77 (d, J_{PC} = 7.6 Hz), 123.90, 123.69 (d, J_{PC} = 3.2 Hz),

dx.doi.org/10.1021/ja501803w | J. Am. Chem. Soc. 2014, 136, 6092−6102

115.08 (d, J_{PC} = 20.9 Hz), 20.95, 18.87 (br, B−CH_2−P), 8.51. ^{31}P{^{1}H} NMR (C_6D_6, 161.967 MHz): δ 46.00. ^{29}Si NMR (C_6D_6, ^{1}H−^{29}Si HMBC: 400 MHz (^{1}H), 79.50 MHz (^{29}Si)): δ 175. IR (cm^{-1}): 1900 (Ru−H), 1618 (Ru−H−Si).

Synthesis of [PhBP$^{Ph}_3$]RuH(η^3-H_2SiMeMes) (1d). A solution of $MesMeSiH_2$ (150 mg, 0.91 mmol) in benzene (1 mL) was added to a dark orange-red solution of **2** (98 mg, 0.059 mmol) in benzene (4 mL). The solution was heated to 60 °C and stirred for 24 h in a flask that was sealed with a threaded Teflon stopper. The resulting amber solution was filtered through Celite, solvent was evaporated under vacuum, and the resulting yellow solid was washed with hexanes (3 × 3 mL) to provide **1d** as an analytically pure, pale yellow powder (84 mg, 74%). Anal. calcd for $C_{55}H_{58}BSiP_3Ru$ (875.86): C, 69.39; H, 6.14. Found: C, 69.45; H, 5.86. ^{1}H NMR (C_6D_6, 600 MHz): 8.14 (d, J = 7.0 Hz, 2 H), 7.68 (t, J = 7.3 Hz, 2 H), 7.52 (br m, 12 H), 7.43 (t, 7.30 Hz, 1 H), 6.86 (t, J = 7.3 Hz, 6 H), 6.80 (t, J = 7.4 Hz, 12 H), 6.59 (2 H), 2.25 (6 H), 2.02 (3 H), 1.82 (br, 6 H, BCH_2P), 1.29 (3 H, Si−Me), −6.80 (m, J_{SiH} = 69 Hz, 3 H, Ru−H). ^{31}P{^{1}H} NMR (C_6D_6, 161.967 MHz): δ 45.97. ^{29}Si NMR (C_6D_6, ^{1}H−^{29}Si HMBC: 400 MHz (^{1}H), 79.50 MHz (^{29}Si)): δ 145.

Synthesis of [PhBP$^{Ph}_3$]Ru[η^3-CH_2(3,5-$Me_2C_6H_3$)] (3). A colorless solution of $(THF)_2MgMes_2$ (39 mg, 0.096 mmol) in benzene (2 mL) was added to a dark orange-red solution of **2** (132 mg, 0.080 mmol) in benzene (2 mL). The resulting dark red solution was stirred for 5 h, after which the solution was filtered through Celite, and solvent was evaporated to give a dark purple solid. The crude product was dissolved in toluene (2 mL), and this solution was layered with pentane and cooled to −35 °C. After 1 week, dark purple crystals had grown. Solvent was removed by pipet, the crystals were washed with pentane (3 × 3 mL), and remaining solvent was evaporated under vacuum to provide **3** as analytically pure, dark purple crystals (131 mg, 90%). Anal. calcd for $C_{54}H_{52}BP_3Ru$ (905.809): C, 71.60; H, 5.79. Found: C, 71.98; H, 6.10. ^{1}H NMR (C_6D_6, 600 MHz): δ 8.10 (br d, J = 7.1 Hz, 2 H), 7.65 (t, J = 7.3 Hz, 2 H), 7.40 (t, J = 7.3 Hz, 1 H), 7.16 (br, 12 H), 6.87 (t, J = 7.3 Hz, 6 H), 6.77 (t, J = 7.3 Hz, 12 H), 6.28 (s, 1 H), 5.14 (s, 2 H), 2.82 (s, 2 H, Ru−CH_2Ar), 1.89 (s, 6 H, Ar(CH_3)$_2$), 1.84 (br, 6 H, B−CH_2−P). ^{13}C{^{1}H} NMR (C_6D_6, 150.893 MHz): 164.59 (br), 149.09, 141.54 (m), 132.90, 132.75, 129.76, 125.16, 124.63, 110.25, 37.48 (q, J_{CP} = 6.4 Hz, Ru−CH_2), 23.21 (Ar(CH_3)$_2$), 18.37 (br, B−CH_2−P). ^{31}P {^{1}H} NMR (C_6D_6, 161.967 MHz): δ 55.6.

Synthesis of [PhBP$^{Ph}_3$]Ru(η^5-C_6H_7) (4). A solution of $EtMe_2SiH$ (85 mg, 0.96 mmol) in benzene (0.5 mL) was added to an orange solution of [PhBP$^{Ph}_3$]Ru(O^{t}Bu) (90 mg, 0.105 mmol) in benzene (1 mL). The solution was stirred for 20 h to give a yellow solution. The solvent was removed under vacuum, and the resulting solids were washed with pentane (3 × 3 mL) and dried under vacuum to provide **4** as an analytically pure off-white powder (81 mg, 89%). Anal. calcd for $C_{51}H_{48}BP_3Ru$ (865.746): C, 70.76; H, 5.59. Found: C, 70.96; H, 5.79. ^{1}H NMR (C_6D_6, 600 MHz): δ 8.10 (d, J = 7.1 Hz, 2 H), 7.60 (t, J = 7.3 Hz, 2 H), 7.38 (t, J = 7.3 Hz, 1 H), 7.34−6.40 (br, 30 H), 5.32 (t, J = 4.4 Hz, 1 H), 5.11 (t, J = 5.7 Hz, 2 H), 2.90 (m, 1 H), 2.72 (t, J = 6 Hz, 2 H), 2.65 (m, 1 H), 2.40−1.40 (br, 6 H). ^{13}C{^{1}H} NMR (C_6D_6, 150.893 MHz): 164.73 (br), 145.24 (br), 132.90 (br), 132.70, 128.92, 128.31, 128.08 (br), 124.60, 97.67, 78.84, 50.08, 28.21 (cyclohexadienyl CH_2 group), 24.32 (br, BCH_2P). ^{31}P {^{1}H} NMR (C_6D_6, 161.967 MHz): δ 39.5.

Synthesis of [PhBP$^{Ph}_3$]Ru[CH_2(2-(η^3-H_2SiMes)-3,5-$Me_2C_6H_2$)] (5). A solution of $(THF)_2Li(SiHMes_2)$ (209 mg, 0.50 mmol) in benzene (1 mL) was added to a stirring suspension of **2** (386 mg, 0.23 mmol) in benzene (10 mL) at room temperature. After stirring for 7 h, the orange suspension was filtered through a plug of Celite. The resulting solution was concentrated under vacuum until a yellow precipitate began forming. The suspension was frozen by cooling to −30 °C. After thawing the mixture, a light orange precipitate settled to the bottom of the suspension, and the cold supernatant was decanted. The light orange solids were washed with pentane (2 × 5 mL) and dried under vacuum to afford analytically pure material (302 mg, 0.29 mmol, 57%). Yellow crystals of **5** could be obtained by vapor diffusion of pentane into toluene solutions of **5** at −30 °C, and a single crystal grown by this method was used for single crystal XRD to determine the solid-state structure of **5**. Anal. calcd for $C_{63}H_{64}BSiP_3Ru$ (1054.07): C, 71.60; H, 6.12. Found: C, 71.88; H, 6.14. ^{1}H NMR (C_6D_6, 600 MHz): δ 8.15 (d, J = 7.3 Hz, 2 H), 7.69 (br t, J = 7.4 Hz, 4 H), 7.64 (t, J = 7.4 Hz, 2 H), 7.43 (br t, J = 7.4 Hz, 4 H), 7.40 (t, J = 7.3 Hz, 1 H), 6.99 (t, J = 7.3 Hz, 4 H), 6.95 (d, J = 7.3 Hz, 4 H), 6.84 (t, J = 7.3 Hz, 4 H), 6.73−6.67 (m, 6 H), 6.63 (1 H), 6.53 (1 H), 6.55 (2 H), 6.49 (t, J = 7.3 Hz, 4 H), 2.91 (br, 2 H, Ru−CH_2Ar), 2.18 (6 H, Ar(CH_3)$_2$), 2.05 (br, 4 H, B−CH_2−P), 2.05 (3 H, ArCH_3), 1.99 (3 H, ArCH_3), 1.97 (3 H, ArCH_3), 1.95 (d, J_{PH} = 12 Hz, 2 H, B−CH_2−P), −7.00 (m, J_{SiH} = 105 Hz, 2 H, Ru−H−Si). ^{13}C{^{1}H} NMR (toluene-d_8, 100.6 MHz): 174.91, 144.80, 144.17, 144.27, 142.00, 141.83, 141.63, 140.84, 140.69, 139.49−138.99 (m), 136.85, 136.76, 135.30, 133.22−133.08 (m), 132.42−132.16 (m), 128.50, 127.38, 127.20, 127.12, 124.11, 32.68 (d, J_{PC} = 41.0 Hz, Ru−CH_2Ar), 24.65, 22.49, 21.38, 21.21, 21.09, 17.46 (br). ^{31}P{^{1}H} NMR (161.967 MHz, C_6D_6): 45.45 (d, J_{PP} = 27 Hz), 25.20 (t, J_{PP} = 27 Hz). ^{29}Si NMR (C_6D_6, ^{1}H−^{29}Si HMBC: 400 MHz (^{1}H), 79.50 MHz (^{29}Si)): δ 138. IR (cm^{-1}): 1674 (Ru−H−Si).

Synthesis of [PhBP$^{Ph}_3$]Ru(CNXyl)(μ-H)=$SiMes_2$ (6). A solution of 2,6-dimethylphenyl isocyanide (XylNC, 13 mg, 0.098 mmol) in toluene (1 mL) was added to a stirring, yellow suspension of **5** (100 mg, 0.095 mmol) in toluene (3 mL) at room temperature. After stirring for 4 h, the bright orange suspension was dried of solvent under vacuum. The resulting orange solids were washed with cold pentane (2 × 5 mL) and dried under vacuum to give **6** as an analytically pure orange powder (87 mg, 0.073 mmol, 77%). Crystallization by vapor diffusion of pentane into a solution of **6** in toluene at −30 °C provided a crystal suitable for structural determination by single crystal XRD analysis. Anal. Calculated: C 72.96%, H 6.21%, N 1.18%; Found: C 73.03%, H 6.39%, N 1.24%. ^{1}H NMR (C_6D_6, 600 MHz): 8.38 (t, J = 8.7 Hz, 2 H), 8.26 (t, J = 8.7 Hz, 2 H), 8.03 (d, J = 7.1 Hz, 2 H), 7.61−7.54 (m, 4 H), 7.35 (t, J = 7.1 Hz, 1 H), 7.20 (t, J = 7.1 Hz, 1 H), 7.18−7.12 (m, 5 H), 7.07 (t, J = 8.7 Hz, 2 H), 6.88 (t, J = 8.7 Hz, 2 H), 6.79 (t, J = 7.4 Hz, 1 H), 6.78−6.70 (br m, 5 H), 6.65 (t, J = 7.4 Hz, 2 H), 6.61−6.52 (m, 5 H), 6.47−6. 42 (m, 4 H), 6.41 (1 H), 6.32 (2 H), 6.30 (1 H), 2.93 (3 H, ArCH_3), 2.86 (3 H, ArCH_3), 2.56 (3 H, ArCH_3), 2.30 (3 H, ArCH_3), 2.18 (m, 1 H, B−CH_2−P), 2.07 (m, 1 H, B−CH_2−P), 2.01 (3 H, ArCH_3), 1.96 (m, 1 H, B−CH_2−P), 1.90 (m, 1 H, B−CH_2−P), 1.82 (m, 1 H, B−CH_2−P), 1.77 (6 H, Ar(CH_3)$_2$), 1.69 (3 H, ArCH_3), 1.67 (m, 1 H, B−CH_2−P), −7.92 (ddd, J_{PH} = 32, 9, 3 Hz, J_{SiH} = 43 Hz, 1 H, Ru−H). ^{13}C{^{1}H} NMR (C_6D_6, 150.893 MHz): 172.25 (dt, J_{CP} = 79, 13 Hz, Ru−CNXyl), 165.59 (br), 145.46, 145.44, 145.22, 145.20, 145.10, 145.08, 144.90, 144.88, 143.65, 143.62, 142.39, 142.17, 142.07, 141.68, 141.41, 141.38, 141.18, 141.15, 140.74, 140.51, 140.09, 138.96, 138.93, 138.25, 138.13, 135.22, 135.11, 135.04, 134.92, 134.84, 133.97, 133.91, 133.79, 133.71, 133.24, 133.18, 133.05, 132.99, 132.60, 129.57, 129.54, 129.50, 129.45, 129.31, 129.22, 128.92, 127.62, 127.47, 127.32, 127.26, 126.99, 126.93, 126.69, 124.42, 27.20, 26.78, 25.27, 24.87, 23.19 (br), 21.74 (br), 21.29, 21.08, 19.33, 17.93 (br). ^{31}P {^{1}H} NMR (C_6D_6, 161.967 MHz): 46.35 (dd, J_{PP} = 21, 39 Hz), 31.80 (dd, J_{PP} = 21, 32 Hz), 24.49 (dd, J_{PP} = 32, 39 Hz). ^{29}Si NMR (C_6D_6, ^{1}H−^{29}Si HMBC: 400 MHz (^{1}H), 79.50 MHz (^{29}Si)): δ 208. IR (cm^{-1}): 2069 (CNXyl), 1996 (Ru−H).

Synthesis of [PhBP$^{Ph}_3$]Ru[CN(2,6-diphenyl-4-methylphenyl)](η^1-(3,5-dimethylbenzyl) (7). A solution of 2,6-diphenyl-4-methylphenyl isocyanide (26 mg, 0.096 mmol) in benzene (1 mL) was added dropwise over 2 min to a stirring solution of **3** (87 mg, 0.096 mmol) in benzene (2 mL). As the isocyanide was added, the color of the solution changed from dark purple to dark red. Solvent was removed under vacuum, and the resulting dark red solid was washed with pentane (3 mL). The crude product was dissolved in toluene (1 mL), layered with pentane, and cooled to −20 °C. After 1 day, dark red crystals had grown, the supernatant was decanted, and the product was washed with pentane (3 × 2 mL) before drying under vacuum to provide **7** as dark red crystals of suitable purity for further synthetic use (108 mg, 96%). Anal. calcd for $C_{74}H_{67}BNP_3Ru$ (1175.155): C, 75.63; H, 5.75; N, 1.19. Found: C, 75.19; H, 6.27; N, 1.17. ^{1}H NMR (C_6D_6, 600 MHz): 8.02 (d, J = 7.5 Hz, 2 H), 7.59 (t,

dx.doi.org/10.1021/ja501803w | J. Am. Chem. Soc. 2014, 136, 6092−6102

J = 7.5 Hz, 2 H), 7.43−7.34 (m, 9 H), 7.24 (t, J = 7.5 Hz, 4 H), 7.22−7.17 (m, 4 H), 7.13 (t, J = 7.5 Hz, 4 H), 6.95 (m, 5 H), 6.83 (t, J = 7.2 Hz, 2 H), 6.80 (2 H), 6.78 (t, J = 7.2 Hz, 2 H), 6.65 (br t, J = 6.9 Hz, 8 H), 6.55 (2 H), 6.27 (t, J = 8 Hz, 4 H), 2.78 (d, J_{PH} = 8.1 Hz, 2 H, Ru−CH_2Ar), 2.28 (6 H, Ar(CH_3)$_2$), 1.93 (3 H, ArCH_3), 1.91 (d, J = 12 Hz, B−CH_2−P), 1.75 (t, J = 13 Hz, 2 H, B−CH_2−P), 1.66 (t, J = 13 Hz, 2 H, B−CH_2−P). $^{13}C\{^1H\}$ NMR (C_6D_6, 150.893 MHz): 175.15 (dt, J_{PC} = 94 Hz, J_{CP} = 12 Hz, Ru−CNAr), 144.63 (d, J_{PC} = 36 Hz), 142.22 (J_{PC} = 34 Hz), 141.08, 140.17, 139.85, 138.52 (d, J_{PC} = 31 Hz), 137.55, 134.59 (J_{PC} = 11 Hz), 134.48, 134.27 (J_{PC} = 10 Hz), 132.68 (J_{PC} = 10 Hz), 132.39, 129.94, 129.71, 128.79, 128.12, 128.06, 127.91 (J_{PC} = 9 Hz), 127.70, 127.68, 124.41, 124.05, 123.75, 31.29 (td, J_{PC} = 15 Hz, J_{PC} = 6 Hz, Ru−CH_2Ar), 24.10 (br, B−CH_2−P), 22.44 (Ar(CH_3)$_2$), 22.08 (br, B−CH_2−P), 21.11 (ArCH_3). $^{31}P\{^1H\}$ NMR (C_6D_6, 161.967 MHz): 46.4 (br), 26.77 (t, J_{PP} = 34 Hz). IR (cm^{-1}): 2037 (CNXyl).

Synthesis of [PhBP$^{Ph}_3$]Ru[CN(2,6-diphenyl-4-methylphenyl)](H)=GeH^{t}Bu (8). Compound **7** (85 mg, 0.072 mmol) was dissolved in a solution of ^{t}BuGeH$_3$ (10 mg, 0.075 mmol) in benzene (1 mL) to give a dark red solution. After stirring for 24 h, the solution had turned orange, and solvent was evaporated under vacuum. The resulting orange solid was washed with pentane (2 mL), dissolved in fluorobenzene (1.5 mL), layered with pentane, and then cooled to −30 °C. After 1 week, this provided analytically pure **8** as orange crystals and yellow microcrystalline powder (68 mg, 79%). A single crystal of **8** suitable for structural determination by XRD analysis was grown by addition of pentane to a solution of **8** in fluorobenzene at room temperature. Anal. calcd for $C_{69}H_{67}BNP_3GeRu$ (1184.823): C, 69.95; H, 5.70; N, 1.18. Found: C, 70.11; H, 5.78; N, 1.10. ^1H NMR (C_6D_6, 600 MHz): 10.74 (br, 1 H, Ge−H), 7.99 (d, J = 6.9 Hz, 2 H), 7.73−7.25 (br, 18 H), 7.09−6.94 (br, 27 H), 1.99 (3 H, ArCH_3), 1.92−1.46 (br, 6 H, B−CH_2−P), 1.21 (9 H, C(CH_3)$_3$), −8.35 (br, 1 H, Ru−H). $^{13}C\{^1H\}$ NMR (C_6D_6, 150.893 MHz): 172.69 (dt, J_{CP} = 79 Hz, J_{CP} = 10 Hz, Ru−CNAr), 165.95, 143.72 (m), 139.48 (br), 137.62, 133.51 (d, J_{CP} = 9 Hz), 133.15 (br), 132.63, 131.88, 130.35 (br), 129.29, 128.05, 127.88 (br), 124.87, 124.31, 28.20, 21.88 (br, B−CH_2−P), 21.27. $^{31}P\{^1H\}$ NMR (C_6D_6, 161.967 MHz): 35.28 (t, J_{PP} = 35 Hz), 33.64 (d, J_{PP} = 35 Hz). IR (cm^{-1}): 2047 (CNXyl), 1900 (Ru−H).

Observation of 1e *in Situ* Upon Addition of H_2 to 5. Complex **5** (6 mg, 0.006 mmol) was dissolved in benzene or C_6D_6 (0.6 mL), and three freeze−pump−thaw cycles were applied to the solution in a J-Young NMR tube. The NMR tube was then filled with an atmosphere of H_2, and the tube was rotated end over end using a slowly rotating motor in order to ensure constant saturation of the solution with H_2. The reaction was monitored by $^{31}P\{^1H\}$ NMR and ^1H NMR spectroscopy, which revealed that **5** was entirely consumed after 20 h and **1e** was formed as the major product (60%). Complex **4** and Mes_2SiH_2 were also formed (30% yield each after 20 h), and after 3 days complex **1e** had entirely decomposed to form **4** and Mes_2SiH_2. Note that addition of D_2 to **5** provided similar results (see Supporting Information). Complex **1e** was not isolated due to its instability, but the ^1H, $^1H\{^{31}P\}$, $^{31}P\{^1H\}$, and $^{29}Si-^1H$ HMBC NMR spectra for **1e** prepared *in situ* provided data that identify **1e** as an η^3-H_2SiMes_2 complex analogous to **1a**−**d**. ^1H NMR (C_6D_6, 600 MHz): 8.12 ppm (d, J = 7.5 Hz, 2 H), 7.65 (t, J = 7.5 Hz, 2 H), (br t, J = 7.7 Hz, 12 H), 7.40 (t, J = 7.5 Hz, 1 H), 6.87 (t, J = 7.4 Hz, 6 H), 6.78 (t, J = 7.4 Hz, 12 H), 6.64 (4 H), 2.47 (12 H), 2.04 (6 H), 1.87 (br, 6 H, BCH_2P), −6.39 ppm (m, 3 H, $^1J_{SiH}$ = 65 Hz, Ru−H and Ru−H−Si), ^{29}Si NMR (C_6D_6, $^1H-^{29}Si$ HMBC: 400 MHz (^1H), 79.50 MHz (^{29}Si)): δ 131 ppm. $^{31}P\{^1H\}$ NMR (C_6D_6, 161.967 MHz): 43.8 ppm.

Catalytic Ge−H Dehydrocoupling of ^{t}BuGeH$_3$ to Form (^{t}BuGeH$_2$)$_2$. ^{t}BuGeH$_3$ (12 mg, 0.090 mmol) was dissolved in benzene-d_6 (0.7 mL) containing C_6Me_6 as an internal standard. An initial ^1H NMR spectrum was collected prior to addition of ∼1 mol % **1b** (1 mg, 0.001 mmol). The initially yellow solution faded to colorless within 5 min, and slow gas evolution was observed. After 10 min, the mixture was examined by ^1H and $^{31}P\{^1H\}$ NMR spectroscopy to reveal 5% conversion of ^{t}BuGeH$_3$ to (^{t}BuGeH$_2$)$_2$ (^1H δ 3.86 ppm, 1.15 ppm) and the release of PhMeSiH$_2$ (^1H δ 4.48 ppm) and H_2 (^1H δ4.46 ppm). After 24 h, an 85% yield of (^{t}BuGeH$_2$)$_2$ was observed (by ^1H NMR), 8% of ^{t}BuGeH$_3$ remained unconverted, and a small amount of higher oligomers may have formed (7%, ^1H δ 4.07−3.97 ppm, 1.23−1.20 ppm). The volatile (^{t}BuGeH$_2$)$_2$ product was not isolated but was characterized in the reaction mixture by ^1H and ^{13}C NMR spectroscopy and GC-MS. ^1H NMR (C_6D_6, 600 MHz): 3.86 (s, 4 H, Ge−H), 1.15 (s, 18 H, C(CH_3)$_3$). $^{13}C\{^1H\}$ NMR (C_6D_6, 150.893 MHz): 31.12, 23.09. GC-MS (note that Ge has wide isotopic distribution) m/z (268, 265, 264, 263, 262, 261, 260, 259, 257) (mixture of M^+, $(M-H)^+$, and $(M-H_2)^+$), 210, 209, 208, 207, 206, 205, 204, 203, 202, 200, 199, 169, 167, 166, 165, 164, 163, 162, 161, 160, 159, 158, 157, 153, 152, 151, 150, 149, 148, 147, 146, 145, 144, 143, 142, 141, 133, 132, 131, 130, 129, 128, 127, 126.

Gas-Phase Exchange of H_2/D_2 between Solid Samples of 1c and 1c-d_3. A sample of **1c**-d_3 (5 mg) was transferred to a small glass test tube and then ground into a fine powder using a spatula. A sample of **1c** (35 mg) was ground into a fine powder using a spatula and then transferred to a glass ampule (20 mL volume). The glass tube containing **1c**-d_3 was placed inside the ampule, and the ampule was then evacuated and flame sealed. After 5 days, the ampule was opened in a nitrogen atmosphere glovebox with care to observe that the deutero sample did not become contaminated with the proteo sample. The sample of **1c**-d_3 was dissolved in C_6D_6 and examined by ^1H NMR spectroscopy, which revealed the presence of an Ru−H resonance that integrated as 0.50 H (compared with 0.14 H for **1c**-d_3 that was not exposed to **1c**).

Transfer of H_2/D_2 through Gas Phase from Solutions of 1b or 1b-d_3 to Solutions of 3. A sample of **1b** or **1b**-d_3 (5−8 mg, 0.005−0.009 mmol) and a sample of **3** (5−8 mg, 0.005−0.009 mmol) were dissolved separately in benzene or benzene-d_6 (1 mL per sample) that contained an internal standard ($Me_3Si)_4Si$ or $Ph_2Si(CH_3)(CD_3)$). The solution of **1b** (or **1b**-d_3) was yellow, and the solution of **3** was dark purple. Preliminary ^1H or ^2H NMR spectra were obtained on the solutions prior to transfer to a Signer molecular weight apparatus that was also charged with two stir bars (one solution and stir bar for each bulb). The solutions were subjected to two freeze−pump−thaw cycles before sealing the apparatus under static vacuum. The solutions were stirred for 3 days and then examined visually and by NMR spectroscopy to reveal the conversion of **1b** (or **1b**-d_3) to **4** and conversion of **3** to mesitylene and **4**. Additional details for these experiments, additional experiments (e.g., using toluene-d_8 as solvent or using the η^3-$H_2SiMeMes$ complex **1d**), and NMR spectra are provided in the Supporting Information.

Computational Details. All calculations were performed using Gaussian 09 suite of programs in the molecular graphics and computing facility of the College of Chemistry, University of California, Berkeley. Calculations were performed using the B3PW91 hybrid functional with the 6-31G(d,p) basis set for all main-group elements and the LANL 2DZ basis set for ruthenium. The crystallographically determined atomic coordinates of **5** and **6** were used as starting points for geometry optimization calculations of **5-DFT** and **6-DFT**. The xylyl isocyanide ligand of **6-DFT** was deleted to create a 16-electron ruthenium silylene structure that was used as a starting point for optimization to the 16-electron silylene structure **silylene-DFT**. Vibrational frequencies were calculated for all converged structures and confirm that these structures lie on minima (no imaginary frequencies were determined). Images and atomic coordinates for all calculated structures are provided in the Supporting Information.

■ ASSOCIATED CONTENT

Supporting Information

Additional experimental and computational details, NMR spectra, and crystallographic information files (cif). This material is available free of charge via the Internet at http://pubs.acs.org.

AUTHOR INFORMATION

Corresponding Author

tdtilley@berkeley.edu

Notes

The authors declare no competing financial interest.

ACKNOWLEDGMENTS

This work was funded by the National Science Foundation under grant no. CHE-1265674. The molecular graphics and computational facility (College of Chemistry, University of California, Berkeley) is supported by the National Science Foundation under grant no. CHE-0840505. We thank Hsueh-Ju Liu for experimental assistance and Andy Nguyen for photography.

REFERENCES

(1) (a) Okazaki, M.; Tobita, H.; Ogino, H. *Dalton Trans.* **2003**, 493–506. (b) Waterman, R.; Hayes, P. G.; Tilley, T. D. *Acc. Chem. Res.* **2007**, *40*, 712–719.

(2) (a) Glaser, P. B.; Tilley, T. D. *J. Am. Chem. Soc.* **2003**, *125*, 13640–13641. (b) Watanabe, T.; Hashimoto, H.; Tobita, H. *J. Am. Chem. Soc.* **2006**, *128*, 2176–2177. (c) Watanabe, T.; Hashimoto, H.; Tobita, H. *J. Am. Chem. Soc.* **2007**, *129*, 11338–11339. (d) Calimano, E.; Tilley, T. D. *Organometallics* **2010**, *29*, 1680–1692. (e) Lee, V. Y.; Aoki, S.; Yokoyama, T.; Horiguchi, S.; Sekiguchi, A.; Gornitzka, H.; Guo, J.-D.; Nagase, S. *J. Am. Chem. Soc.* **2013**, *135*, 2987–2900.

(3) (a) Harrod, J. F. *Inorganic and Organometallic Polymers*, ACS Symposium Series 360; Zeldin, M., Wynne, K. J., Allcock, H. R., Eds.; American Chemical Society: Washington, DC, 1988; pp 89–100. (b) Harrod, J. F.; Ziegler, T.; Tschinke, V. *Organometallics* **1990**, *9*, 897–902.

(4) Schneider, N.; Finger, M.; Haferkemper, C.; Bellemin-Laponnaz, S.; Hofmann, P.; Gade, L. H. *Angew. Chem., Int. Ed.* **2009**, *48*, 1609–1613.

(5) (a) Mitchell, G. P.; Tilley, T. D. *Angew. Chem., Int. Ed.* **1998**, *37*, 2524–2526. (b) Mitchell, G. P.; Tilley, T. D. *J. Am. Chem. Soc.* **1998**, *120*, 7635–7636. (c) Ochiai, M.; Hashimoto, H.; Tobita, H. *Angew. Chem., Int. Ed.* **2007**, *43*, 8192–8194.

(6) (a) Peters, J. C.; Feldman, J. D.; Tilley, T. D. *J. Am. Chem. Soc.* **1999**, *121*, 9871–9872. (b) Mork, B. V.; Tilley, T. D. *J. Am. Chem. Soc.* **2001**, *123*, 9702–9703. (c) Watanabe, T.; Hashimoto, H.; Tobita, H. *Angew. Chem., Int. Ed.* **2004**, *43*, 218–221.

(7) (a) Corey, J. Y.; Braddock-Wilking, J. *Chem. Rev.* **1999**, *99*, 175–292. (b) Corey, J. Y. *Chem. Rev.* **2011**, *111*, 863–1071.

(8) (a) Gusev, D. G.; Fontaine, F.-G.; Lough, A. J.; Zargarian, D. *Angew. Chem., Int. Ed.* **2003**, *42*, 216–219. (b) Corriu, R. J. P.; Lanneau, G. F.; Chauhan, B. P. *Organometallics* **1993**, *12*, 2001–2003.

(9) Alacarez, G.; Helmstedt, U.; Clot, E.; Vendier, L.; Sabo-Etienne, S. *J. Am. Chem. Soc.* **2008**, *130*, 12878–12879.

(10) Lipke, M. C.; Tilley, T. D. *J. Am. Chem. Soc.* **2011**, *133*, 16374–16377.

(11) Note that the proteo sample of **1c** was used in excess (7 equiv) to accelerate the rate of H_2 exchange in to the deuetero sample **1c**. Thus, the percentage change in the Ru–H resonance and incorporation of deuterium into Ru–D positions were comparatively small for the proteo sample of **1c** and not suitable for measurement by NMR spectroscopy.

(12) *o*-Dichlorobenzene was the highest boiling solvent used for this experiment. *o*-Dibromobenzene was investigated, but samples of **1a–d** decomposed rapidly in this solvent prior to applying vacuum.

(13) The decomposition was evident from the formation of an insoluble species that was not observable by NMR spectroscopy.

(14) Brown, S. D.; Peters, J. C. *J. Am. Chem. Soc.* **2004**, *126*, 4538–4539.

(15) A Signer apparatus typically used for molecular weight determination was utilized for this experiment, see Zoellner, R. W. *J. Chem. Educ.* **1990**, *67*, 714–715.

(16) For the picture in Figure 1, aqueous solutions of $KMnO_4$ and Na_2CrO_4 were used in place of actual solutions of **3** and **1b,d**. Note that actual solutions of **3** are a somewhat duller, red-purple color in comparison with the color of the $KMnO_4$ solution.

(17) Iluc, V. M.; Hillhouse, G. L. *J. Am. Chem. Soc.* **2010**, *132*, 11890–11892.

(18) Mitchell, G. P.; Tilley, T. D. *Organometallics* **1998**, *17*, 2912–1916.

(19) (a) Simmons, R. S.; Gakat, K. J.; Bradshaw, J. D.; Youngs, W. J.; Tessier, C. A.; Allón, G.; Alvarez, S. *J. Organomet. Chem.* **2001**, *628*, 241–254. (b) Sakaba, H.; Hirata, T.; Kabuto, C.; Kabuto, K. *Organometallics* **2006**, *25*, 5145–5150.

(20) (a) Sadow, A. D.; Tilley, T. D. *J. Am. Chem. Soc.* **2002**, *124*, 6814–6815.

(21) (a) Brammer, L.; Klooster, W. T.; Lemke, F. R. *Organometallics* **1996**, *15*, 1721–1727. (B) Duncan, J. L.; Harvie, J. L.; McKean, D. C.; Cradock, S. *J. Mol. Struct.* **1986**, *145*, 225–242.

(22) For the longest previously reported Ru=Si distance: Takaoka, A.; Mendirata, A.; Peters, J. C. *Organometallics* **2009**, *28*, 3744–3753.

(23) DFT calculations were performed with Gaussian 09 using the B3PW91 functional and LANL2DZ/6-31G** basis sets for Ru/main group elements, respectively.

(24) (a) Nakata, M.; Fujita, T.; Sekiguchi, A. *J. Am. Chem. Soc.* **2006**, *128*, 16024–16025. (b) Watanabe, C.; Iwamoto, T.; Kabuto, C.; Kira, M. *Angew. Chem., Int. Ed.* **2008**, *47*, 5386–5389.

(25) Hayes, P. G.; Beddie, C.; Hall, M. B.; Waterman, R.; Tilley, T. D. *J. Am. Chem. Soc.* **2006**, *128*, 428–429.

(26) (a) Litz, K. E.; Henderson, K.; Gourley, R. W.; Banaszak Holl, M. M. *Organometallics* **1995**, *14*, 5008–5010. (b) Bender, J. E., IV; Litz, K. E.; Giarikos, D.; Wells, N. J.; Banaszak Holl, M. M.; Kampf, J. W. *Chem.–Eur. J.* **1997**, *3*, 1793–1796. (c) Reichl, J. A.; Popoff, C. M.; Gallagher, L. A.; Remsen, E. E.; Berry, D. H. *J. Am. Chem. Soc.* **1996**, *118*, 9430–9431. (d) Katz, S. A.; Reichl, J. A.; Berry, D. H. *J. Am. Chem. Soc.* **1998**, *120*, 9844–9849.

(27) (a) Hayes, P. G.; Waterman, R.; Glaser, P. G.; Tilley, T. D. *Organometallics* **2009**, *28*, 5082–5089. (b) Fasulo, M.; Tilley, T. D. *Chem. Commun.* **2012**, *48*, 7690–7692.

(28) Cordero, B.; Gómez, V.; Platero-Prats, A. E.; Revés, M.; Echeverría, J.; Cremades, E.; Barragán, F.; Alvarez, S. *Dalton Trans.* **2008**, 2832–2838.

(29) Almon, M. J.; Doncaster, A. M; Noble, P. N. *J. Am. Chem. Soc.* **1982**, *104*, 4717–4718.

(30) Roddick, D. M.; Heyn, R. H.; Tilley, T. D. *Organometallics* **1989**, *8*, 324–330.

(31) Kerr, W. J.; Watson, A. J. B.; Hayes, D. *Chem. Commun.* **2007**, 5049–5051.

(32) Ito, H.; Kato, T.; Sawamura, M. *Chem. Asian J.* **2007**, *2*, 1436–1446.

(33) Betley, T. A.; Peters, J. C. *Inorg. Chem.* **2003**, *42*, 5074–5084.

(34) Lipke, M. C.; Tilley, T. D. *J. Am. Chem. Soc.* **2013**, *135*, 10298–10301.